Preparation of core/shell structured NiO-based ceramics and their dielectric properties

2005 J. Phys. D: Appl. Phys. 38 1615

(http://iopscience.iop.org/0022-3727/38/10/017)

INSTITUTE OF PHYSICS PUBLISHING JOURNAL OF PHYSICS D: APPLIED PHYSICS

J. Phys. D: Appl. Phys. **38** (2005) 1615–1620 doi:10.1088/0022-3727/38/10/017

Preparation of core/shell structured NiO-based ceramics and their dielectric properties

Yuanhua Lin, Lei Jiang, Rongjuan Zhao, Gang Liu and Ce-Wen Nan[1]

State Key Laboratory of New Ceramics and Fine Processing, Department of Materials Science and Engineering, Tsinghua University, Beijing, 100084, People's Republic of China

E-mail: cwnan@tsinghua.edu.cn

Received 17 January 2005, in final form 16 March 2005
Published 6 May 2005
Online at stacks.iop.org/JPhysD/38/1615

Abstract

High-permittivity dielectric core/shell structured $Li_{0.01}Si_xNi_{0.99-x}O$ ceramics (abbreviated as LSNO) have been successfully prepared. Analyses of the ceramic microstructure and composition indicate that the dopants of SiO_2 are mainly dispersed into the grain boundaries and exist as the insulating Ni_2SiO_4 phase. All the LSNO ceramic samples exhibit high permittivity, and the permittivity reaches about 1.2×10^4 for the LSNO-1 sample. The concentration of Si has a remarkable effect on the dielectric properties of the LSNO ceramics. The origin of the high permittivity observed in these LSNO ceramics is attributed to the Maxwell–Wagner polarization mechanism and a thermally activated mechanism.

1. Introduction

Recently, a great deal of intensive research has been conducted on high-permittivity dielectric materials for their use in microelectronics devices, such as capacitors and memory devices [1, 2]. The high dielectric permittivities are usually observed in perovskite ferroelectric oxides, e.g. $Pb(Zr,Ti)O_3$ (PZT) and $Pb(Mg,Nb)O_3$ (PMN) [3, 4]. Another perovskite-related material $CaCu_3Ti_4O_{12}$ (CCTO) with an unusually high permittivity of $\sim 10^4$–10^5 at room temperature has been reported [5–7]. It was considered that the origin of the large dipole moments in CCTO could be due to the interfacial polarization mechanism, and no ferroelectric transition akin to those in high-permittivity perovskites has been observed. Lunkenheimer *et al* [8] discussed that many colossal permittivity (CDC) observations are not intrinsic in origin, and concluded that most of the CDCs reported so far are based on Maxwell–Wagner-type extrinsic effects due to contact effects, and grain boundary (GB) effects in ceramic samples. Additionally, boundary layer capacitors (BLCs) based on semiconductive perovskite oxides such as $SrTiO_3$ have also attracted attention. These BLC ceramics are normally processed in the reductive and partial oxidative atmosphere so that grains of the oxides become semiconducting while GBs are insulating [9, 10]. At present, high-capacitance ceramic capacitors with BLC and MLCC (multilayer ceramic capacitors) structures are the potential trend for obtaining high-density charge storage [11, 12].

In this report, a non-ferroelectric and non-perovskite high-permittivity core/shell structured material, $Li_{0.01}Si_xNi_{0.99-x}O$ (LSNO) ceramic, has been successfully synthesized. The high dielectric permittivity behaviour observed in rocksalt-type LSNO is similar to that observed recently in perovskite-like CCTO. It was suggested that the high permittivity response of LSNO could arise from the Maxwell–Wagner polarization (i.e. interfacial polarization) mechanism and thermally activated mechanisms, such as charge carrier transport, rather than due to permanent dipoles. The LSNO-based ceramic shows high permittivity, which makes such simple compounds attractive for BLC applications and challenges the supremacy of $BaTiO_3$-based compositions, which involve a complex multistage process, e.g. involving high temperatures, reducing atmospheres, and limited diffusion of oxygen and dopant ions in the grain boundaries.

[1] Author to whom any correspondence should be addressed.

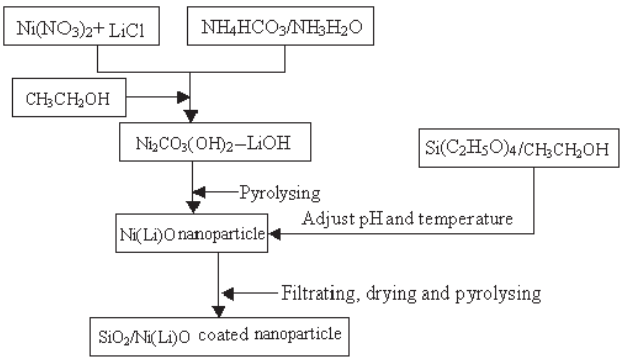

Figure 1. Schematic processing technology of coated SiO_2/NiO particles.

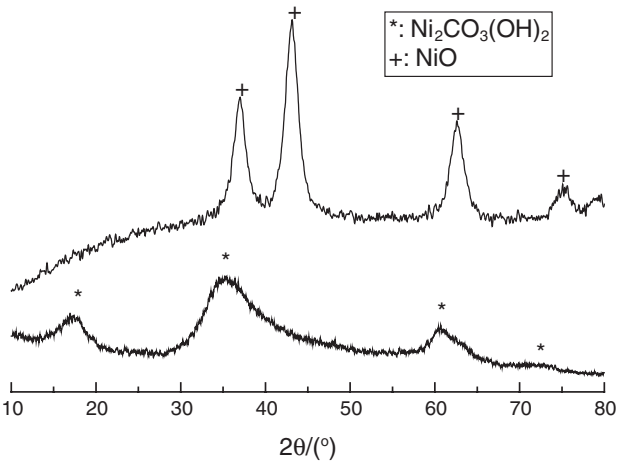

Figure 2. Typical XRD patterns of LSNO-2 composites and its calcined powders.

2. Experimental

$Ni(NO_3)_2{\cdot}6H_2O$ (A.R.), $LiNO_3$ (A.R.), $Si(C_2H_5O)_4$ (A.R.) and CH_3CH_2OH were employed as raw materials. The specimens with nominal compositions $Li_{0.01}Si_{0.05}Ni_{0.94}O$ (LSNO-1), $Li_{0.01}Si_{0.15}Ni_{0.84}O$ (LSNO-2) and $Li_{0.01}Si_{0.25}Ni_{0.74}O$ (LSNO-3) were prepared as shown in figure 1. Stoichiometric amounts of $Ni(NO_3)_2{\cdot}6H_2O$ and $LiNO_3$ were first mixed and dissolved in an appropriate amount of distilled water to get the clear solution, then added into a $NH_3{\cdot}H_2O$–NH_4HCO_3 buffer solution at about 70°C, and the mixture was agitated continuously till the $Ni_2CO_3(OH)_2$–LiOH composite precipitate formed. The Ni(Li)O nanosized powders were obtained by the decomposition of the above carbonate precursor at 400°C for 2 h, and the nanosized Ni(Li)O particles were dispersed into CH_3CH_2OH–H_2O solution. Later $Si(C_2H_5O)_4$–CH_3CH_2OH solution was added slowly into the above suspending solution, and then the solution was heated and stirred to form the gel. The amorphous SiO_2/Ni(Li)O coated nanoparticles were obtained after the dried gel was calcined at 800°C for 1 h in air. Then, the resultant LSNO powders were pressed to form green pellets 10 mm in diameter and about 1.2–1.8 mm in thickness at a pressure of 10 MPa by using polyvinyl alcohol as a binder. Three LSNO ceramic samples (LSNO-1: Φ9.8 mm × 1.3 mm, LSNO-2: Φ9.7 mm × 1.7 mm and LSNO-3: Φ9.5 mm × 1.8 mm) were prepared via traditional ceramic processing and sintered at 1250°C for 2 h in air. The sintered ceramic samples were polished, and electroded by silver paint on both sides of the disc-shaped samples fired at 650°C for 30 min for dielectric permittivity measurements.

X-ray diffraction (XRD), transmission electron microscopy (TEM) with selected area electron diffraction (SAED), high-resolution transmission electron microscopy (HRTEM) and scanning electron microscopy (SEM) equipped with energy dispersive spectroscopy (EDS) were employed to reveal the microstructure and phase composition of the LSNO ceramics. Dielectric permittivity measurements were conducted in an evacuated dielectric cell. The dielectric response of the specimens was measured using a HP 4192A gain phase analyser over a frequency range from 100 Hz to 1 MHz and at an oscillation voltage of 1.0 V.

3. Results and discussion

Three kinds of LSNO ceramic samples with nominal compositions $Li_{0.01}Si_{0.05}Ni_{0.94}O$ (LSNO-1), $Li_{0.01}Si_{0.15}Ni_{0.84}O$ (LSNO-2) and $Li_{0.01}Si_{0.25}Ni_{0.74}O$ (LSNO-3) have been synthesized with the technology flow shown in figure 1 combined with traditional ceramic processing. As shown in figure 2, the phase composition of as-prepared typical LSNO-2 precursor powders includes the $Ni_2CO_3(OH)_2$ phase, and the Li precipitates (e.g. LiOH, Li_2CO_3) cannot be observed in the patterns due to the small doping amount. The $Ni_2CO_3(OH)_2$ phase was changed to the NiO phase after pyrolysing the composites at 400°C for 2 h. The resultant particles are the core/shell structured amorphous SiO_2/ Ni(Li)O nanoparticles. The amorphous SiO_2 shell and Ni(Li)O core can obviously be observed in the TEM, HRTEM and SAED patterns shown in figure 3, and the average particle size of NiO and thickness of the amorphous SiO_2 are 70 nm and 10 nm, respectively. As shown in figures 4 and 5, the original shell/core structured particles can be transformed into new grain/GB structured Ni_2SiO_4/ Ni(Li)O particles after sintering at 1250°C for 2 h. The SEM micrographs imply that the core Ni(Li)O grains have grown to be approximately 2.0 μm in the LSNO-2 ceramic sample, and the dopants of SiO_2 are mainly dispersed into the grain boundaries, as proved by the EDS results shown in table 1.

Figure 6 shows the frequency dependence of the permittivity ε of the LSNO samples at room temperature. The permittivity values at 100 Hz for the LSNO-1, LSNO-2 and LSNO-3 samples are 12 375, 6750 and 4964, respectively. The ε value for the LSNO-1 sample is found to be nearly 600 times larger than that for the pure NiO sample.

Normally, pure stoichiometric NiO is an excellent insulator, with a room temperature resistivity of about $\sim 10^{13}$ Ω cm, but introduction of Ni^{2+} vacancies and/or doping with monovalent cations like Li^+ can cause considerable increase in the conductivity of NiO, and the conduction in NiO is mainly due to thermal excitation of the mobilities (small-polaron hopping) [13, 14]. Since the ionic radius of Li^+ is almost identical to that of Ni^{2+}, the majority of Li^+ impurities will substitute for the Ni^{2+} site. Since the second ionization potential of Li is 40 eV larger than the third ionization potential

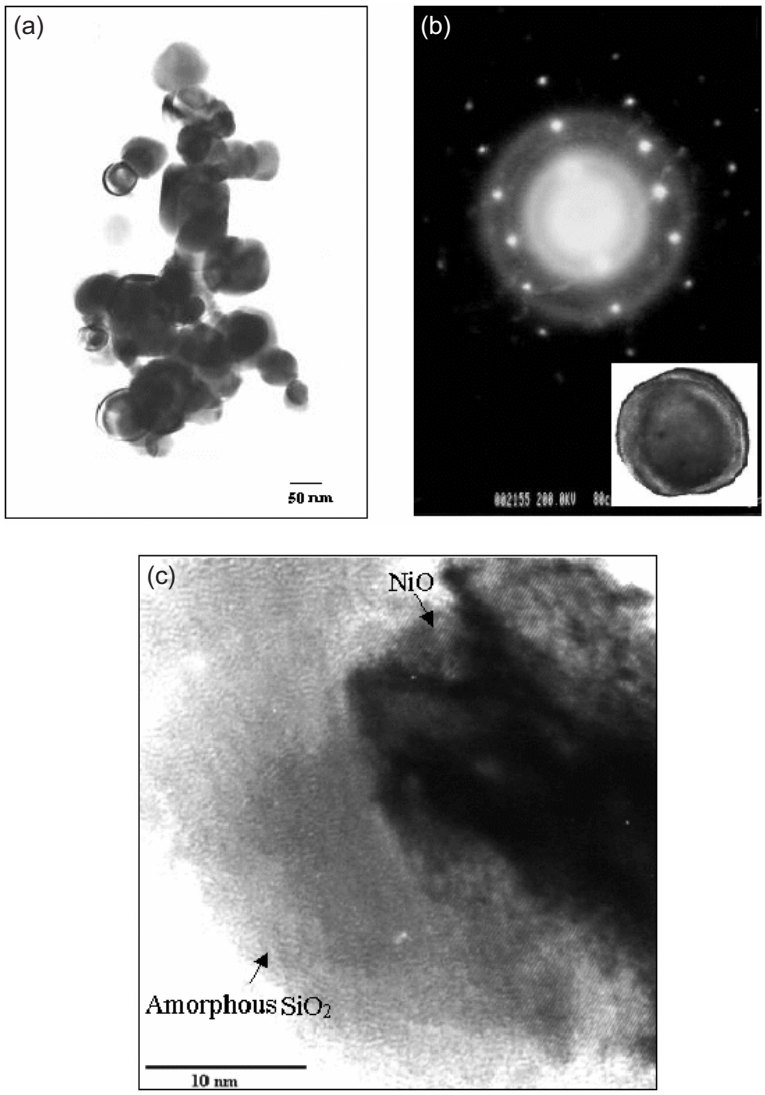

Figure 3. TEM, SAED and HRTEM micrographs of LSNO-2 precursor particles. (*a*) TEM micrographs, (*b*) SAED patterns and (*c*) HRTEM micrographs.

of Ni, charge neutrality is achieved by forming a Ni^{3+} ion for every Li^+ ion introduced into the lattice [15]. Since a Ni^{3+} ion is a Ni^{2+} ion with an extra hole, Li^+ impurities act as acceptors and the conduction is p type and dominated by the free holes in the 2p band. Additionally, due to the addition of SiO_2, one part of SiO_2 reacted with NiO to form the Ni_2SiO_4 phase dispersing into the GB as shown in figure 4 and table 1, and another part entered into the NiO grains and substituted for the Ni site, which resulted in the formation of Ni vacancies as follows:

$$SiO_2 \xrightarrow{NiO} Si_{Ni}^{\bullet\bullet} + V_{Ni}'' + 2O_o^x. \tag{1}$$

As an electric field was applied, two types of hopping processes can occur in the LSNO system, i.e. the long-range inter-well hopping and the short range intra-well hopping of holes [16]. The frequency and temperature dependence of the inter-well and intra-well hopping mechanisms are markedly different from one another, and each has its respective contribution to the dielectric properties in the LSNO samples. When an ac field is applied, both inter-well and intra-well hopping mechanisms do have a finite probability of occurrence, and their relative probabilities are dependent on the energy of the charge carriers, frequency of the applied signal and concentration, mean site separation, depth and extent of percolation of the potential wells.

As shown in figure 6, it can be seen that the permittivity and dielectric loss decrease with increasing frequency. This behaviour may be explained qualitatively by the assumption regarding the mechanism of the polarization process. The LSNO ceramics can be regarded as a dielectric material with high concentration of hopping charge carriers. The large values of ε at low frequencies in dielectrics with a high density of hopping charge carriers may be understood on the basis of the definition of polarization as the dipole moment per unit volume [17].

$$p = \sum_{\alpha} \chi_\alpha q_\alpha, \tag{2}$$

where α takes into account all charged particles in the system, q represents the respective charges and χ the displacement under an applied electric field.

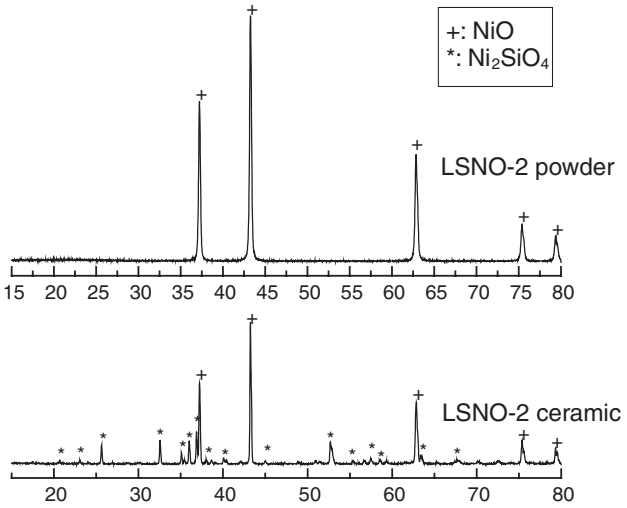

Figure 4. XRD patterns of LSNO-2 powder particles and as-sintered products at 1250°C for 2 h.

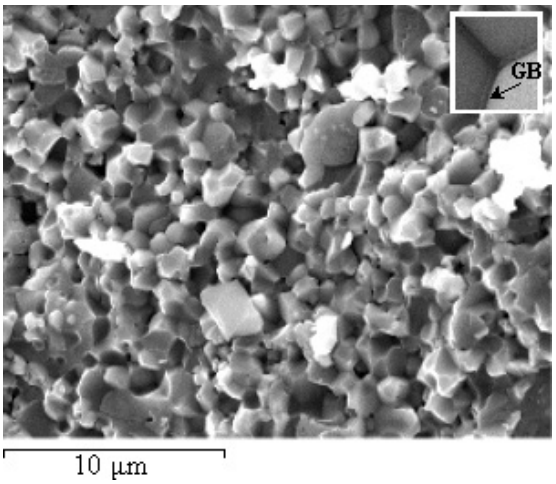

Figure 5. SEM micrographs of fractured surface for LSNO-2 ceramics.

Table 1. The results of EDS for the LSNO-2 sample.

	Fractured surface of grain		Grain boundary	
Element	Weight%	Atomic%	Weight%	Atomic%
O	8.79	25.30	15.38	35.68
Si	3.64	5.97	15.70	20.75
Ni	87.58	68.73	68.92	43.57
Si/Ni		0.08		0.48

According to the correlated Barrier Hopping model [18], the inter-well hopping is the predominant process at low frequencies. Normally, inter-well hopping corresponding to the steady-state transport of charge carriers between the electrodes does not contribute to polarization [19]. However, in the LSNO samples, owing to the high density of defects (e.g. V''_{Ni}) concentrated at the highly disordered GBs, there will be a reasonable extent of percolation of adjacent defect potential wells, and the inter-well hopping also contributes to dielectric relaxation at low frequencies. Thus, large values of ε can be observed for all the LSNO samples at low frequencies. As the signal frequency is increased to higher values, the probability of occurrence of intra-well hopping becomes large since the charge carriers do not get enough time for long-range hopping before field reversal. At higher frequencies (e.g. in the 1 MHz range), the charge carriers would barely have started to move before the field alters its direction, and therefore, the permittivity of LSNO ceramics may decrease substantially as the frequency increases.

Normally, the Maxwell–Wagner polarization, also known as the interfacial polarization, often arises in a material consisting of grains separated by more insulating inter-grain barriers [20]. The Maxwell–Wagner polarization model has been successfully employed to explain the dielectric relaxation with extremely high permittivity ceramics [21, 22] (e.g. CCTO, $BaFe_{1/2}Nb_{1/2}O_3$, $Gd_{0.6}Y_{0.4}BaCo_2O_{5.5}$). The common interpretation assumes a whole series of boundary barriers and grains, or even a series–parallel array of boundary barriers, which arises if the material consists of grains separated by more insulating inter-grain barriers as in boundary layer capacitors.

As previously reported [23], the resistivity of NiO can be improved by doping by monovalent cations to several orders of magnitude. The core/shell structured LSNO ceramics consist of well-conducting grains, Ni(Li)O and nonconducting or poorly conducting GB layers (e.g. Ni_2SiO_4). Consider the grain and GB to have different permittivities (ε_1 and ε_2) and different conductivities (σ_1 and σ_2), so that the complex permittivities in the LSNO ceramics can be described as

$$\varepsilon_1^* = \varepsilon_1 - \frac{\mathrm{i}\sigma_1}{\omega}, \tag{3}$$

$$\varepsilon_2^* = \varepsilon_2 - \frac{\mathrm{i}\sigma_2}{\omega}. \tag{4}$$

The total permittivity can be quantitatively approximated by [22]:

$$\varepsilon^* = \frac{L}{d(\varepsilon_1^*)^{-1} + t(\varepsilon_2^*)^{-1}}. \tag{5}$$

Here, d is the particle size of the conducting grain (core), and t is the thickness of the GB (shell), $L = t + d$. Since $t \ll L$, $\sigma_1 \ll \sigma_2$, equation (5) can be simplified as follows:

$$\begin{aligned}\varepsilon^* &= \frac{\varepsilon_1}{(1 + (d\varepsilon_1/L\varepsilon_2))} + \frac{\varepsilon_2}{(d/L)(1 + (d\varepsilon_1/L\varepsilon_2))}\frac{1}{1 + \mathrm{i}\omega\tau} \\ &= \frac{\varepsilon_1}{\xi} + \frac{\varepsilon_2}{\xi\delta}\frac{1}{1 + \mathrm{i}\omega\tau},\end{aligned} \tag{6}$$

where $\xi = 1 + \delta\varepsilon_1/\varepsilon_2$, $\tau = \xi\varepsilon_2/\delta\sigma_1$, $\delta = d/L$.

At zero or very low frequency, equation (6) can be further simplified as

$$\varepsilon^* = \frac{L\varepsilon_2}{d}. \tag{7}$$

Then equation (7) indicates that the permittivity is controlled by the thin nonconducting layer. As for the LSNO ceramics, the average Ni(Li)O grain size is about 2.0 μm, and the thickness of the GB region with increasing doping SiO_2 is estimated to be about 5–15 nm, and the permittivity of Ni_2SiO_4 is about 30 [24]. Therefore, the permittivity at low frequency will be 4000–12 000, which is in good agreement with our experimental data.

Additionally, high dielectric loss in the low frequency region can also be observed, which is probably ascribed

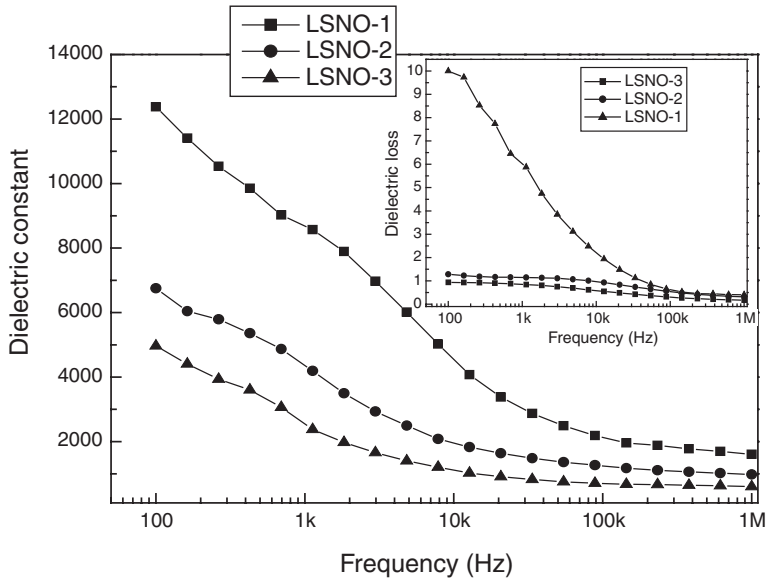

Figure 6. Frequency dependence of permittivity and loss for various LSNO ceramics.

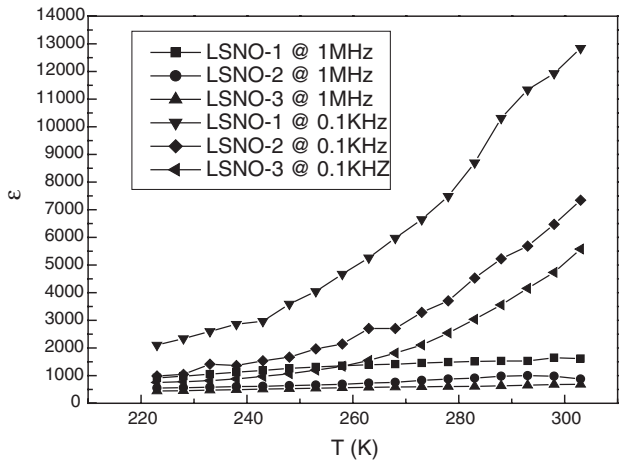

Figure 7. Temperature dependence of permittivity for various LSNO ceramics.

to the following: in the low frequency region, inter-well hopping corresponding to the steady-state conduction is the predominant process. Due to the overlapping of the defect potential wells, only a small fraction of the total number of holes executing long-range hopping reverse direction on field reversal to contribute to polarization, while the majority of the holes contribute to energy loss due to steady-state charge transport between the electrodes, which was also observed in the nanosized NiO materials [25].

The temperature dependence of the permittivity at 1 KHz and 1 MHz for LSNO ceramics is shown in figure 7. The variation of the permittivity with frequency is small at low temperatures and at high frequencies. In the absence of a field, the charge carriers that are bounded at different localized states would show different dipole orientations. A hole can hop between a pair of these centres under the action of an ac field, leading to the re-orientation of an electric dipole. This process would give rise to a change in the permittivity. Figure 7 clearly shows the permittivity increase with increase in the temperature over the entire frequency range for all the samples, which indicates that the polarization is partially due to some thermally activated mechanisms, such as charge carrier transport rather than due to permanent dipoles. This is in agreement with our discussion on the dielectric relaxation mechanism and observed frequency response based on hopping of holes. Actually, the activation energy E_g of these three LSNO samples' grains (e.g. LSNO-2 $\sim$ 0.201 eV), fitted by the reverse temperature dependence of the dc conductivity, as in the polaron theory, is nearly equal to E_a (e.g. LSNO-2 $\sim$ 0.195 eV) fitted by the dependence of dielectric loss on temperature at various frequencies (the activation energy required for relaxation), which indicates that the polarization relaxation is closely related to the conductivity in the grain interior. A detailed analysis will be the subject of a future publication [26].

4. Conclusions

Three kinds of high-permittivity dielectric core/shell structured LSNO ceramics have been successfully prepared by chemical synthesis combined with traditional ceramic processing. The doping amount of SiO_2 has great influence on the dielectric properties due to the thickness of the GB, and the permittivity varies from 10^3 to 10^4 at low frequency, which is in good agreement with the calculated results. The high dielectric loss is caused by the holes contributing to energy loss due to steady-state charge transport between the electrodes. The high dielectric response can be ascribed to the Maxwell–Wagner polarization mechanism and thermally activated mechanism.

Acknowledgments

This work was supported by the Ministry of Sci & Tech of China through a 973-Project, under grant No 2002CB613303; and National High Technology Research and Development Program of China, under grant No 2003AA302120 and the National Natural Science Foundation.

References

[1] Spearing S M 2000 *Acta Mater.* **48** 179
[2] Lin Y H *et al* 2004 *J. Am. Ceram. Soc.* **87** 742
[3] Swartz S L *et al* 1984 *J. Am. Ceram. Soc.* **67** 311
[4] Kim B G, Cho S M, Kim T Y and Jang H M 2001 *Phys. Rev. Lett.* **86** 3404
[5] Homes C C, Vogt T, Shapiro S M and Wakimoto S 2001 *Science* **293** 673
[6] He L, Neaton J B and Cohen M H 2002 *Phys. Rev.* B **65** 214112
[7] Cohen M H *et al* 2003 *J. Appl. Phys.* **94** 3299
[8] Lunkenheimer P *et al* 2002 *Phys. Rev.* B **66** 52105
[9] Yang C F 1996 *Japan. J. Appl. Phys.* **35** 1806
[10] Takeshima Y, Shiratsuyu K, Takagi H and Sakabe Y 1997 *Japan. J. Appl. Phys.* **36** 5870
[11] Pecharroman C, Fatima Esteban-Bategon and Jose S Moya 2001 *Adv. Mater.* **13** 1541
[12] Haertling G H 1999 *J. Am. Ceram. Soc.* **82** 797
[13] Van Elp J, Eskes H, Kuiper P and Sawatzky G A 1992 *Phys. Rev.* B 45 1612
[14] Terkura K, Williams A R and Oguchi T 1984 *Phys. Rev. Lett.* **52** 1830
[15] Adler D and Feinleib J 1979 *Phys. Rev.* B **2** 3112
[16] Biju V and Khadar M A 2001 *Mater. Res. Bull.* **36** 21
[17] Jonscher A K 1978 *J. Mater. Sci.* **13** 553
[18] Bosman A J and Van Daal H J 1970 *Adv. Phys.* **19** 1
[19] Sayer M, Mansingh A, Webb J B and Noad J 1978 *J. Phys. C: Solid State Phys.* **11** 315
[20] Ross Macdonald J 1987 *Impedance Spectroscopy* (New York: Wiley)
[21] Bobnar V *et al* 2002 *Phys. Rev.* B **65** 184403
[22] Raevskia I P *et al* 2003 *J. Appl. Phys.* **93** 4130
[23] Bosman A J 1965 *Phys. Rev.* B **144** 763
[24] Xu T X 1993 *Electronic Ceramics* (Tianjin: Tianjin University Press)
[25] Biju V and Khadar M A 2003 *J. Mater. Sci.* **38** 4055
[26] Lin Y H, Jiang L, Zhao R and Nan C-W 2005 *Phys. Rev.* B submitted